Journal Homepage: - www.journalijar.com

INTERNATIONAL JOURNAL OF ADVANCED RESEARCH (IJAR)

Article DOI: 10.21474/IJAR01/10154
DOI URL: http://dx.doi.org/10.21474/IJAR01/10154

RESEARCH ARTICLE

NEW APPROACH BASED ON ANALYTIC-NUMERICAL METHOD FOR CALCULATING THE SLIDING DISTANCE OF TEETH PROFILE POINTS DURING GEARS MESHING.

N. Agbetossou[1], D. Koffi[2], K. Attipou[1], S. Tiem[3] and A. Afio[1].

1. Département de Génie Mécanique, Ecole Nationale Supérieure d'Ingénieurs, Université de Lomé, B.P. 1515 Lomé, Togo.
2. Centre de recherche en Matériaux Ligno Cellulosiques, Département de génie mécanique, Ecole d'ingénierie, Université du Québec à Trois-Rivières, CP 500, Trois-Rivières, Québec, G9A 5H7, Canada.
3. Professeur Titulaire, Département de Génie Mécanique, Ecole Nationale Supérieure d'Ingénieurs, Université de Lomé, B.P. 1515.

Manuscript Info

Manuscript History
Received: 03 October 2019
Final Accepted: 05 November 2019
Published: December 2019

Key words:
Gear, Sliding Distance, Tooth Profile, Hertz Deformation, Matlab.

Abstract

New approach based on analytic-numerical method for calculating the sliding distance of teeth profile points during gears meshing is proposed in this study. In our approach we have shown that the sliding distance of teeth profile points is due to the Hertz deformation. Our method of calculation consist of following a point on the profile by its radius during the contact. The analytical approach has been successfully implemented in Matlab code and solved numerically. The results show that the sliding distance is not null at pitch point. Compared with the common used method, the results are very close, except at the neighborhoods of the pitch point and the points of the head and the foot, where the deviations become greater. The deviations for normal points vary between 0.16% and 6.52% for simulated meshing conditions.

Introduction:-

Gear transmission is one of the most used means of transmission. In gear transmissions, there is a relative slip between the two profiles in contact due to the very kinematics of the gear transmission mechanism. This slip associated with the load and the speed generates the friction, the intense heating and the wear of the profiles in contact and impacts the performance of the gears.

Wear is one of the modes of gear failure and in addition it affects other modes of damage [1, 2]. According to the Archard model wear laws [2, 3, 6, 12] developed for the gears, the wear rate is directly related to the contact pressure, to the sliding distance of each point of contact and tribo-mechanical characteristics (coefficient of friction, lubrication condition, hardness or Young's modulus) of the materials in contact.

The experimental results agree well with those of the models, for the metallic gears, with a zero wear rate at the pitch point. The zero wear rate at the pitch point is explained by a sliding distance of zero at this point, since theoretically the sliding speed is zero. As calculated to date, the approximate formula for calculating the sliding distance gives a zero value at the pitch point [2, 3, 6].

Corresponding Author:- N. Agbetossou.
Address:- Département de Génie Mécanique, Ecole Nationale Supérieure d'Ingénieurs, Université de Lomé, B.P. 1515 Lomé, Togo.

Apart from the approximate method commonly used by all, the literature on this subject is almost non-existent. Only Anders Flodin [6] approached the problem differently, but he did not propose a concrete formula for generalized use. Just recently in 2015, Zhao et al [10,11] proposed an analytic formula, but it too is not directly usable. Most other authors have often circumvented the problem by the numerical integral or finite element method of infinitesimal sliding distance [1, 12, 13]. The latter approach is often appropriate to the particular cases treated.

However, unlike metal gears, the experimental wear tests results for plastic gears show a non-zero wear rate at the pitch point, rather it is considerable [4,5]. The method of the approximate formula giving a zero sliding distance at the pitch point proves to be inappropriate with the models based on Archard's law, for the prediction of the wear of the plastic gears.

This observation has led us in our research work on the laws of prediction of the gears wear in plastic materials and their composites, to develop an analytical-numerical method for calculating this sliding distance of the points of the profiles during meshing.

This work includes, in the first place, a review on the modeling of the meshing, followed by a theoretical analysis of the sliding distance during the meshing, then a numerical simulation is done using the Matlab software. The results from the simulation are presented and analyzed and finally comes a conclusion to finish.

Theoretical analysis of sliding distance during meshing:-
The modeling of the gears meshing:-
Characteristic data:-

Table 1:- Below presents the characteristic data of the meshing modeling.
Table 1:- Parameters of the meshing modeling.

Parameters	Pignion	Gear	Parameters	Pignon	Gear
Nomber of teeth	Z_1	Z_2	Pitch circle	d_1, R_1	d_2, R_2
Module	m	m	Base circle	d_{b1}, R_{b1}	d_{b2}, R_{b2}
Diametral pitch	D_P=25.4/m	DP=25.4/m	Outside circle	d_{a1}, R_{a1}	d_{a2}, R_{a2}
Pressure angle	α	α	Root circle	d_{f1}, R_{f1}	d_{f2}, R_{f2}
Rotation speed	$\boldsymbol{\omega}_1$	$\boldsymbol{\omega}_2$	Cicular pitch	$p = m\pi$	$p = m\pi$
Addendum	h_a=m	h_a=m	Base pitch (p_b ou p_n)	$p_n = m\pi\cos\alpha$	$p_n = m\pi\cos\alpha$
Dedendum	h_f = 1.25m	h_f = 1.25m	Center distance	$a = m(Z_1 + Z_2)/2$	$a = m(Z_1 + Z_2)/2$
Clearrance	c = 0.25m	c = 0.25m			

Principle of gears meshing and normalized reference:-
Figure 1a summarizes the principle for a meshing of spur gear. Here the driving gear rotates clockwise.

Figure1a:- Principle of gears meshing O_2

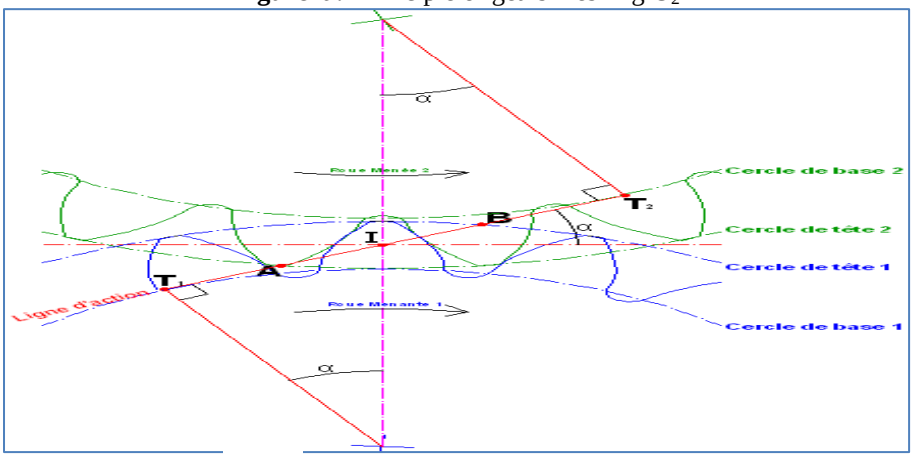

The point A is the beginning of theoretical contact between a pair of teeth with conjugate profiles.

The point B is the end of theoretical contact between the same pair of teeth with conjugate profiles.

A and B are the intersections of the outside circles with the action line. The contact point of the tooth profiles describes the segment [AB] where [AI] is the approach segment and [IB] the recess segment.

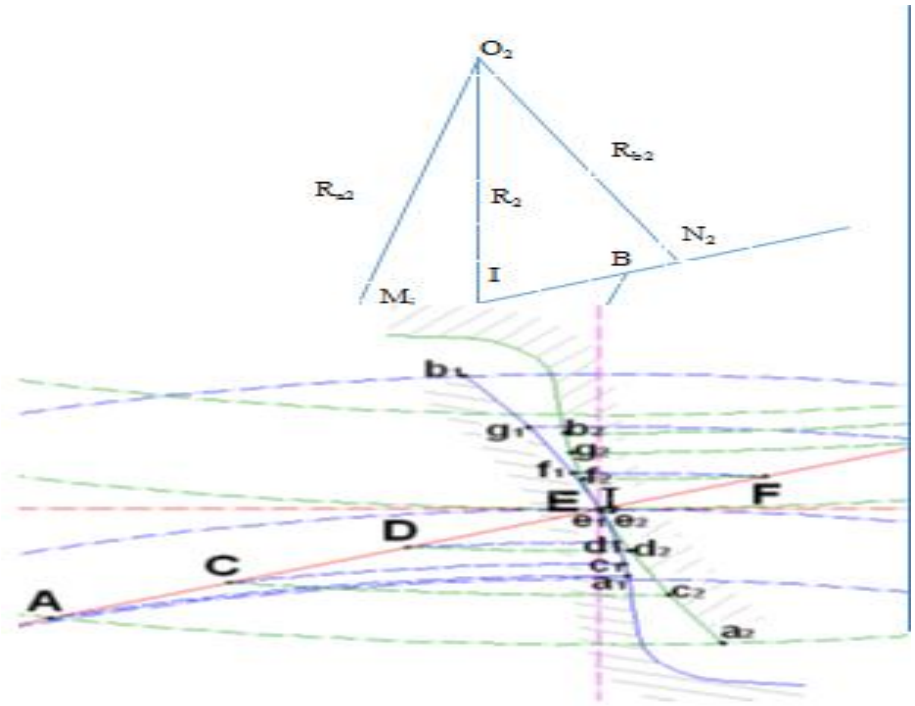

Figure 1 c:- Principle of gears meshing.

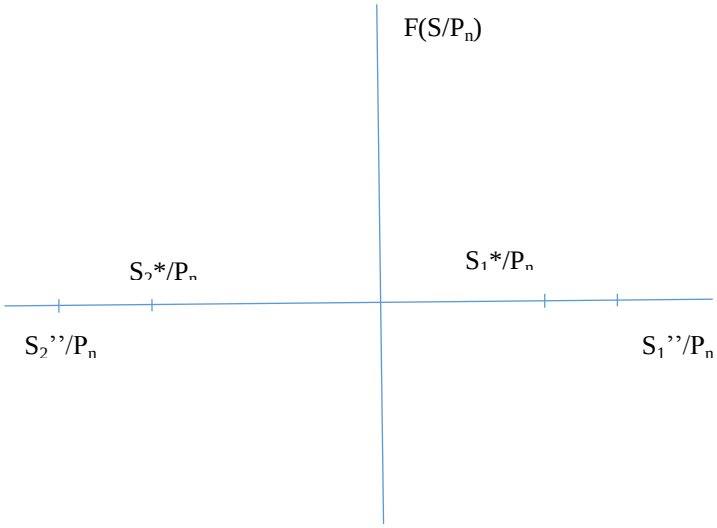

Figure1c:- Principle of gears meshing.

Figure 1c shows how the conjugate points on the two profiles come into contact on the line of act.ion. Figure 1b and Figure 2 show the relationships between the normalized positions and the corresponding points on the profiles. They also make it possible to calculate the geometrical data of the meshing.

In the normalized reference, the position of the theoretical contact start point is $\frac{S_2^*}{P_n}$, the real contact start point is $\frac{S_2''}{P_n}$, the position of the end of the theoretical contact is $\frac{S_1^*}{P_n}$, and the end of the real contact is $\frac{S_1''}{P_n}$. For the metal-to-metal meshing, the theoretical beginning and the real beginning are practically confounded, so the theoretical end and the real end of contact are also practically confounded. The formulas for calculating its different positions will be established later.

Calculation of geometrical data:-

Referring to the characteristic data and figures 1b and 2, we have:-

$R_1 = \frac{mZ_1}{2}$ (1); $R_2 = \frac{mZ_2}{2}$ (2);

$R_{a1} = R_1 + m$ (3); $R_{a2} = R_2 + m$ (4);

$R_{b1} = R_1 \cos\alpha$ (5); $R_{b2} = R_2 \cos\alpha$ (6);

$R_{f1} = R_1 - 1.25m$ (7); $R_{f2} = R_2 - 1.25m$ (8);

$N_1I = \sqrt{R_1^2 - R_{b1}^2}$ (9); $N_2I = \sqrt{R_2^2 - R_{b2}^2}$ (10);

$AI = AN_2 - IN_2 = \sqrt{R_{a2}^2 - R_{b2}^2} - R_{b2} tg\alpha$ (11) ;

$IB = N_1B - N_1I = \sqrt{R_{a1}^2 - R_{b1}^2} - R_{b1} tg\alpha$ (12) ;

The contact ratio is given by:

$$CR = \varepsilon_\alpha = \frac{\sqrt{\left(\frac{d_{a1}}{2}\right)^2 - \left(\frac{d_{b1}}{2}\right)^2} + \sqrt{\left(\frac{d_{a2}}{2}\right)^2 - \left(\frac{d_{b2}}{2}\right)^2} - \left(\frac{d_{b1}}{2} + \frac{d_{b2}}{2}\right)\tan\alpha}{\pi m \cos\alpha} \quad (13);$$

As defined by the normalized reference, we have:

$\frac{S_2^*}{P_n} = \frac{-AI}{m\pi\cos\alpha}$ (14); $\frac{S_1^*}{P_n} = \frac{IB}{m\pi\cos\alpha}$ (15);

For gears in thermoplastic materials there is an extension of the contact before and after the beginning and the end of the theoretical contact [3]. We have indeed:

$$\frac{s_2''}{P_n} = \frac{s_2^*}{P_n} - \delta\frac{s_2}{P_n} \quad (16)$$

$$\frac{s_1''}{P_n} = \frac{s_1^*}{P_n} + \delta\frac{s_1}{P_n} \quad (17)$$

Where for a plastic/plastic meshing:

$$\frac{\delta s_2}{P_n} = \frac{\delta s_1}{P_n} = \frac{\delta s}{P_n} = 0.131.E_2^{-0.34}\left(Z_2\sqrt{W_0.P.\cos\alpha}\right)^{0.7}.\left(\frac{Z_2}{Z_1}\right)^{-0.55} \quad (18)$$

And for a metal/plastic meshing:

$$\frac{\delta s_i}{P_n} = \frac{\delta s}{P_n}.\left(\frac{E_1}{E_2}\right)^{\theta} \quad (19)$$

i = 2 θ = -0.11

i = 1 θ = -0.05

With s_2''/P_n and s_1''/P_n the normalized positions on the action line for beginning and end of real contact, s_2^*/P_n, s_1^*/P_n normalized positions on the action line for beginning and end of theoretical contact, E_1, E_2 the Young modulus for the pinion and gear in Ib/po^2, α the pressure angle, W_0 the normal load per unit width of the teeth in Ib/po and P the diametral pitch.

For the contacts between the beginning and the theoretical end we have:-

For a normalized position $\frac{S_i}{P_n}$ in approach:-

$$R_{i1} = \sqrt{R_{b1}^2 + (N_1I + \frac{S_i}{P_n}\pi m\cos\alpha)^2} \quad (20);$$

$R_{i2} = \sqrt{R_{b2}^2 + (N_2 I + \frac{S_i}{P_n}\pi m cos\alpha)^2}$ (21);

For a normalized position $\frac{S_j}{P_n}$ in recess:

$R_{j1} = \sqrt{R_{b1}^2 + (N_1 I + \frac{S_j}{P_n}\pi m cos\alpha)^2}$ (22);

$R_{j2} = \sqrt{R_{b2}^2 + (N_2 I + \frac{S_j}{P_n}\pi m cos\alpha)^2}$ (23);

Kinematics data:-

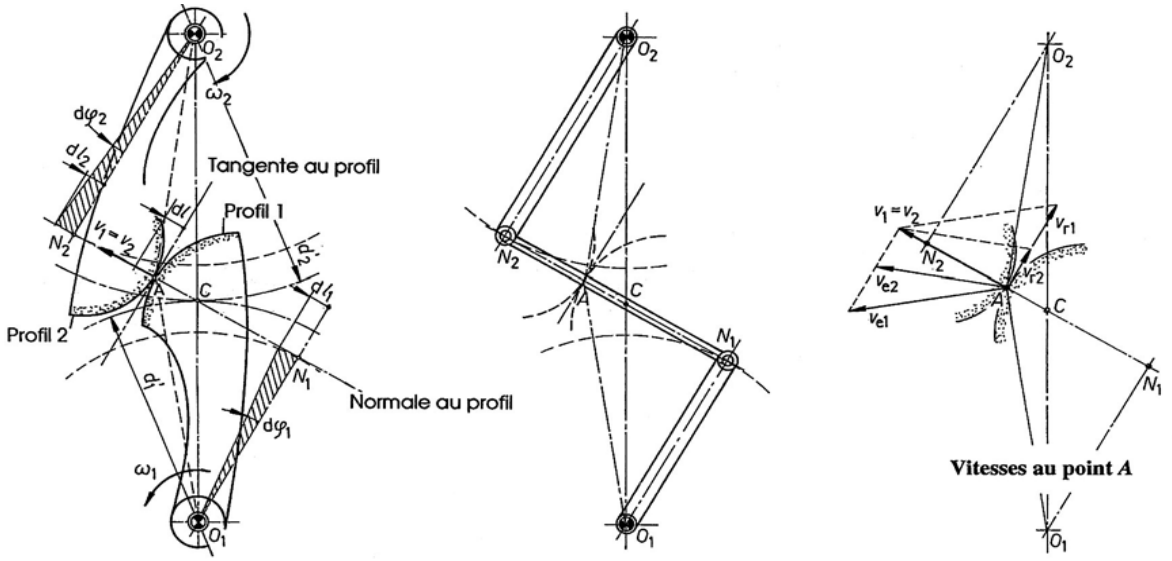

Figure 3:- Simulation by substitution cam and articulated linkage system for gear meshing kinematic

The cinematic of the meshing is nowadays well known. There are different approaches and different formulas but all give the same results. Using the velocity composition law, at contact point M_i (here A in the figure) on the line of action, we have the following kinematic data:-

Relative velocities across the common tangent of the two profiles, V_{r1i} and V_{r2i} at the point of contact, such as:-

$V_{r1i} = \omega_1 N_1 M_i = \omega_1 \left(N_1 I + \frac{S_i}{P_n}\pi m cos\alpha\right)$ (24);

$V_{r2i} = \omega_1 N_2 M_i = \omega_1 \left(N_2 I - \frac{S_i}{P_n}\pi m cos\alpha\right)$ (25);

The relative velocities of the point M_i come from the rotation of the profiles around the instantaneous points N_1 and N_2. The rolling speeds of the profiles with respect to the points N_1 and N_2 have the same intensity as the relative speeds, but are of opposite directions [7].

The sliding velocities V_{g1i} and V_{g2i} are such that:

$V_{g1i} = V_{r1i} - V_{r2i}$ (26);

$V_{g2i} = V_{r2i} - V_{r1i}$ (27);

- The absolute velocities V_1 and V_2 are such that:

$V_1 = V_2 = \omega_1 R_{b1} = \omega_2 R_{b2} = V$ (28);

- The slip ratios which are the ratios of the sliding speeds over the rolling speeds are such that:

$\gamma_{1i} = \frac{V_{g1i}}{V_{r1i}}$ (29);

$\gamma_{2i} = \frac{V_{g2i}}{V_{r2i}}$ (30).

Static and dynamic data:-
radius of curvature

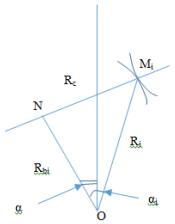

Figure 4- Radius of curvature

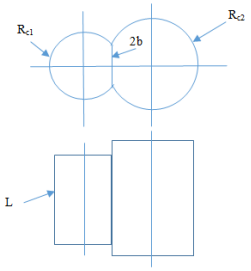

Figure 5- Deformation of Hertz

For involute profiles, for any point of the profile, the center of curvature is always the tangent point of the line of action with the base circle.

When a pair of tooth is in contact and under the effect of the load, the deformation of Hertz spreads over 2b and the contact is made on a rectangle of width 2b and length L.
The radius of curvature is given by:-
$\alpha_i = cos^{-1}\left(\frac{R_b}{R_i}\right)$ (31);
$R_{ci} = R_i \, sin\, \alpha_i$ (32);
Ou bien Or
$R_{ci} = \sqrt{R_i^2 - R_b^2}$ (33);
The reduced radius is given by:
$\frac{1}{R_{ci}} = \frac{1}{R_{c1i}} + \frac{1}{R_{c2i}}$ (34);
b- Load distribution factor

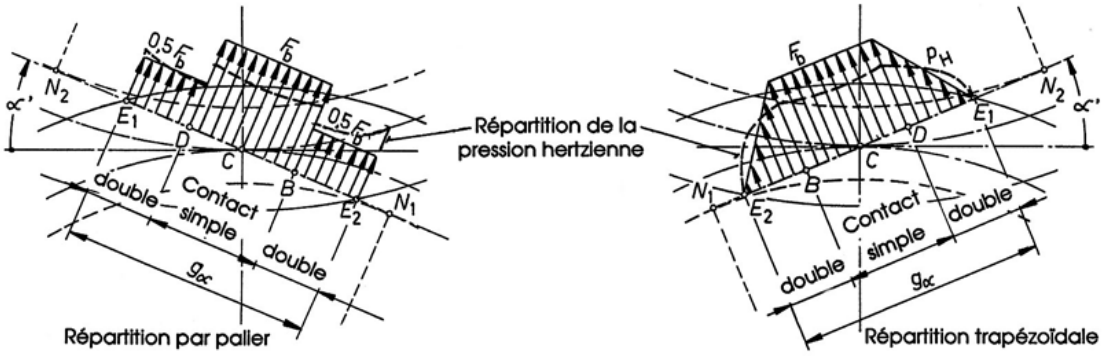

Figure 6:- Distribution of normal load for metal/metal meshing.

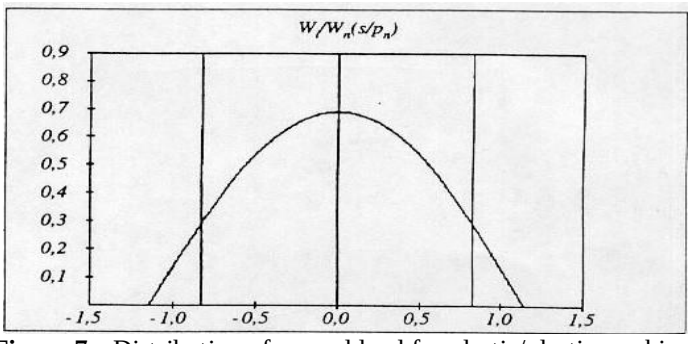

Figure 7:- Distribution of normal load for plastic/plastic meshing.

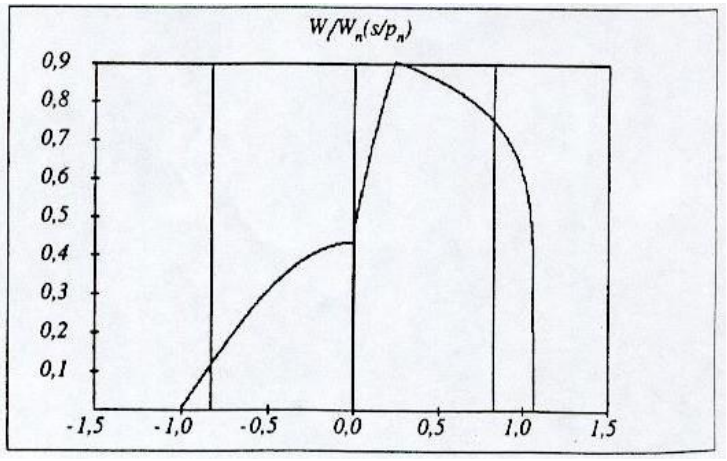

Figure 8:- Distribution of normal load for metal/plastic meshing.

This being so, for any type of meshing (metal/metal, plastic/plastic or plastic/metal), it is known to determine for each meshing position on the line of action, the load supported by each tooth.

For the case of plastic/plastic meshing which interests us more particularly in this study, we have:

$$\frac{W_i}{W_n}\left(\frac{s}{P_n}\right) = \left.\frac{W_i}{W_n}\right|_0 .\cos\left(\frac{\pi}{2}.\frac{s/P_n}{s_2''/P_n}\right) \quad (35)$$

with :

$$\left.\frac{W_i}{W_n}\right|_0 = 0.48.E_2^{-0.28}.\left(W_0.P.\cos\alpha\right)^{-0.22}.Z_2^{-0.4}.\left(\frac{Z_2}{Z_1}\right)^{0.1} \quad (36)$$

Where $\left.\frac{W_i}{W_n}\right|_0$ is the value of the load distribution factor at the pitch point (s = 0).

W_n is the total load following the action line transmitted to all the teeth in contact.

W_i is the load transmitted along the line of action to the main tooth meshing at the Si position.

c- Calculation of the half-width of Hertz.

At the contact in the position S_i, we have:

$$b_i = \left[\frac{4W_i}{\pi L}\cdot\frac{\frac{1-\upsilon_1^2}{E_1}+\frac{1-\upsilon_2^2}{E_2}}{\frac{1}{R_{c1i}}+\frac{1}{R_{c2i}}}\right]^{1/2} \quad (37);$$

E_1 and E_2 are respectively Young modulus of the pinion and the gear materials;

υ_1 and υ_2 are respectively Poisson coefficient of the pinion and the gear materials.

Theoretical analysis of the calculation of the sliding distance of each point of the tooth profiles in meshing:-

For this study, we limit ourselves between the beginnings of theoretical contact A and the end of theoretical contact B on the action line. This is the reality of metal gears. For gears made of polymeric materials, a similar study will be made for contact before point A and contact after point B.

The references and parameters calculation are defined in Figures 9, 10, 11 and 12.

The reference (I, x, y) consists of the axis (I, y) which is the straight line linking the centers O_1 O_2 of the two gears, and the axis (I, x) perpendicular to the axis (I , y). The angle between the action line (A, B) and the axis (I, x) is the pressure angle α.

Figure 9 shows the contact at point A and the contact at point B.
If we consider that a pair of teeth come into contact at point A, then immediately after the contact, because of the sudden Hertz deformation, the points of profile 1 of the driving tooth, from A towards its top over the half -Hertz contact length b, come all into contact at the same time with the profile 2 of the driven tooth.

Similarly, the points of the profile 2 of the driven tooth, from its top R_{a2} towards the base, on the half-contact length of Hertz b, come all into contact at the same time with the profile 1 of the driving tooth.

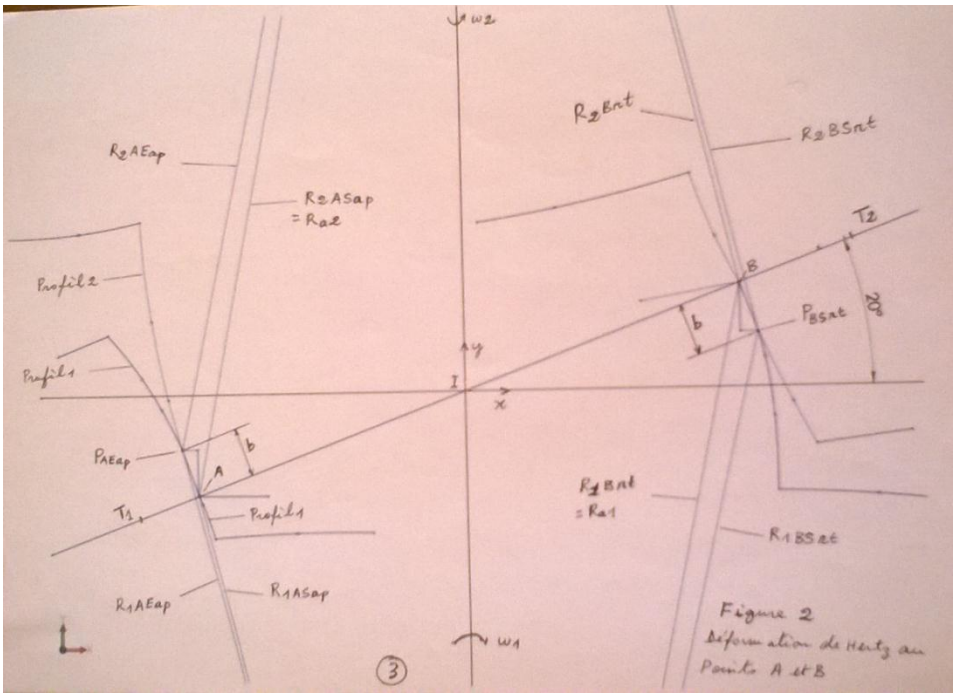

Figure 9:- Hertz deformation at starting point A and at ending point B of gears meshing.

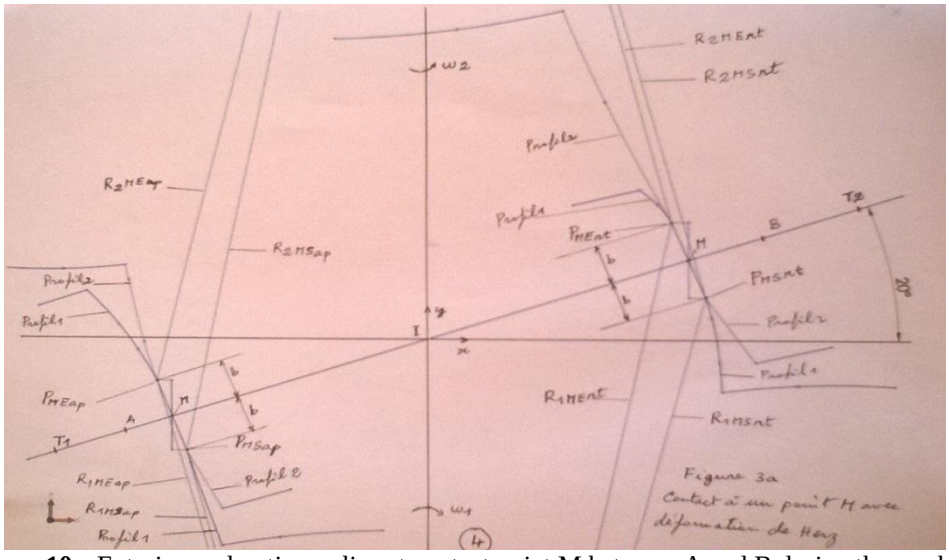

Figure 10:- Entering and outing radius at contact point M between A and B during the meshing

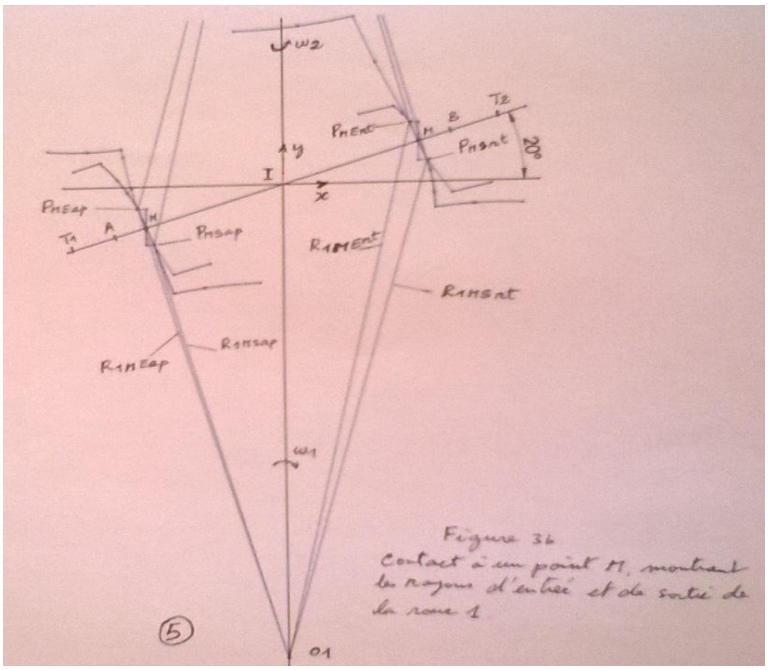

Figure 11:- Entering and outing radius at contact point M on profil1 during meshing.

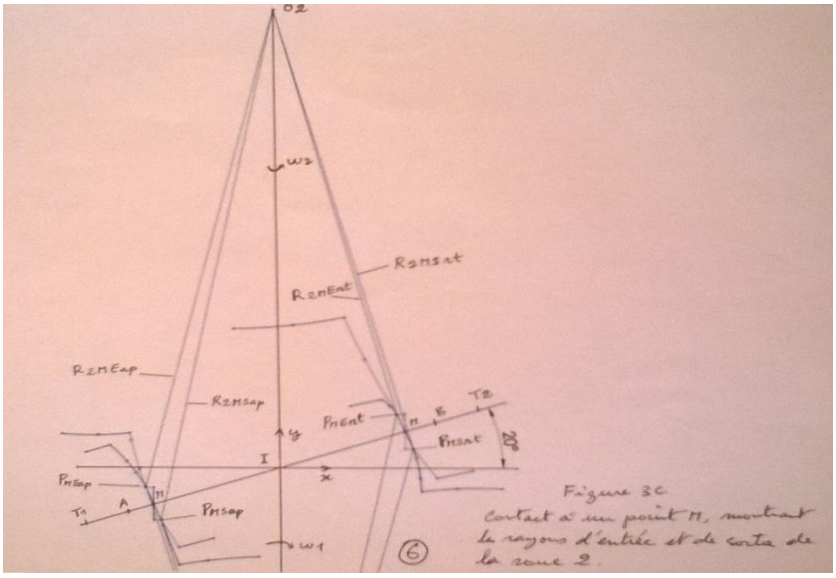

Figure 12:- Entering and outing radius at contact point M on profil2 during meshing.

Similar to point B, the points of the profile 1 of the driving tooth, from its vertex Ra1 towards the base, on the half contact length of Hertz b, come all out of the contact at the same time and the points of the profile 2 of the driven tooth, from B to the top on the half-contact length of Hertz b, come all out of the contact at the same time.

Apart from the edge cases at A and B, at each meshing position M between A and B, a pair of points (R_{1ME}, R_{2ME}) comes into contact and another pair of points (R_{1MS}, R_{2MS}) leaves the contact (Figure 10, 11, 12).
We obtain the following formulas:

In approach between A and I, at the point of contact M, we obtain in the reference (I, x, y):

$$M\begin{cases} X_M = -IM\cos\alpha \\ Y_M = -IM\sin\alpha \end{cases} (41) ;$$

$P_{ME}\begin{cases}X_{ME} = X_M - b_M sin\alpha \\ Y_{ME} = Y_M + b_M cos\alpha\end{cases}$ (42) ; then $\begin{cases}R_{1ME} = \sqrt{X_{ME}^2 + (R_1 + Y_{ME})^2} \\ R_{2ME} = \sqrt{X_{ME}^2 + (R_2 - Y_{ME})^2}\end{cases}$ (43) ;

$P_{MS}\begin{cases}X_{MS} = X_M + b_M sin\alpha \\ Y_{MS} = Y_M - b_M cos\alpha\end{cases}$ (44) ; then $\begin{cases}R_{1MS} = \sqrt{X_{MS}^2 + (R_1 + Y_{ME})^2} \\ R_{2MS} = \sqrt{X_{MS}^2 + (R_2 - Y_{ME})^2}\end{cases}$ (45) ;

In recess between I and B, at the point of contact M, we obtain in the reference (I, x, y):

$M\begin{cases}X_M = IM cos\alpha \\ Y_M = IM sin\alpha\end{cases}$ (46) ;

$P_{ME}\begin{cases}X_{ME} = X_M - b_M sin\alpha \\ Y_{ME} = Y_M + b_M cos\alpha\end{cases}$ (47) ; then $\begin{cases}R_{1ME} = \sqrt{X_{ME}^2 + (R_1 + Y_{ME})^2} \\ R_{2ME} = \sqrt{X_{ME}^2 + (R_2 - Y_{ME})^2}\end{cases}$ (48) ;

$P_{MS}\begin{cases}X_{MS} = X_M + b_M sin\alpha \\ Y_{MS} = Y_M - b_M cos\alpha\end{cases}$ (49) ; then $\begin{cases}R_{1MS} = \sqrt{X_{MS}^2 + (R_1 + Y_{ME})^2} \\ R_{2MS} = \sqrt{X_{MS}^2 + (R_2 - Y_{ME})^2}\end{cases}$ (50) ;

In approach and in recess, the formulas are verified in the neighborhood of point I.

b_M is the half contact length of Hertz at the point of contact M. It is known to calculate b_M, which varies with the normal load at each meshing position.

Our method of calculation consists of following a point J of the profile by its radius R_{M1E} which comes into contact at the position M_1 and which leaves the contact at the position M_2 by its radius R_{M1S} ($R_{M1E} = R_{M1S}$).

Since the meshing motion over AB is uniform, the point M moves at a constant speed over AB ($V_M = R_{b1}\omega_1 = R_{b2}\omega_2$).

So, the sliding time of point J is: $\Delta t_J = \frac{M_1M_2}{V_M}$ (51).

As the sliding speed is uniformly decelerated in approach [AI] and uniformly accelerated in recess [IB], we have:

$d_J = \frac{1}{2}(V_{jgE} + V_{jgS})\frac{M_1M_2}{V_M}$ (52), if M_1 and M_2 belong to [AI] or to [IB], if not,

$d_J = \frac{1}{2}\left(\frac{M_1I}{V_M}V_{jgE} + \frac{IM_2}{V_M}V_{jgS}\right)$ (53) ;

with V_{jgE} the module of the entering sliding speed of point J and V_{jgS} the module of the outing sliding speed of point J.

Numerical simulation:-

We will make a separate mesh for the [AI] approach and for [IB] recess.

In approach, we make the mesh in N_1 following positions:

$\frac{S_i[1]}{P_n} = \frac{S_2^*}{P_n} = \frac{-AI}{m\pi\cos\alpha}$ (54);

$\frac{S_i[N1]}{P_n} = 0$ (55); (the position of the pitch point I).

We set, the mesh step in approach,

$P_a = \frac{-AI}{m\pi\cos\alpha.(N_1-1)}$; (56) ;

For i = 2 à N_1-1 ;

$\frac{S_i[i]}{P_n} = \frac{S_i[1]}{P_n} - P_a.(i-1)$ (57);

Then, the formula: $M\begin{cases}X_M = -IM cos\alpha \\ Y_M = -IM sin\alpha\end{cases}$ (41); becomes: $M_i\begin{cases}X_M[i] = m\pi\cos\alpha\frac{S_i[i]}{P_n}cos\alpha \\ Y_M[i] = m\pi\cos\alpha\frac{S_i[i]}{P_n}sin\alpha\end{cases}$ (58);

In recess, we make the mesh in N_2 following positions:

$\frac{S_j[N2]}{P_n} = \frac{S_1^*}{P_n} = \frac{-IB}{m\pi\cos\alpha}$ (59);

$\frac{S_j[1]}{P_n} = 0$ (60); (the position of the pitch point I).

We set, the mesh step in recess,

$P_r = \frac{IB}{m\pi\cos\alpha.(N_2-1)}$; (61) ;

For j = 2 à N_2-1 ;

$\frac{S_j[j]}{P_n} = \frac{S_j[1]}{P_n} + P_r.(j-1)$ (62);

Then, the formula: M $\begin{cases} X_M = -IMcos\alpha \\ Y_M = -IMsin\alpha \end{cases}$ (46); becomes: M_j $\begin{cases} X_M[j] = m\pi\ cos\ \alpha \frac{S_j[j]}{P_n} cos\alpha \\ Y_M[j] = m\pi\ cos\ \alpha \frac{S_j[j]}{P_n} sin\alpha \end{cases}$ (63) ;

With a computer program, all the input radius $R_{1ME[i]}$ or $R_{1ME[j]}$ and $R_{2ME[i]}$ or $R_{2ME[j]}$ are computed, the set of output radius $R_{1MS[i]}$ or $R_{1MS[j]}$ and $R_{2MS[i]}$ or $R_{2MS[j]}$, as well as their relative velocities and corresponding input and output sliding velocities. By identifying the input assembly and the output assembly, the sliding distance of several representative positions is then calculated according to the desired accuracy and the sliding distance curve is constructed in the normalized reference.

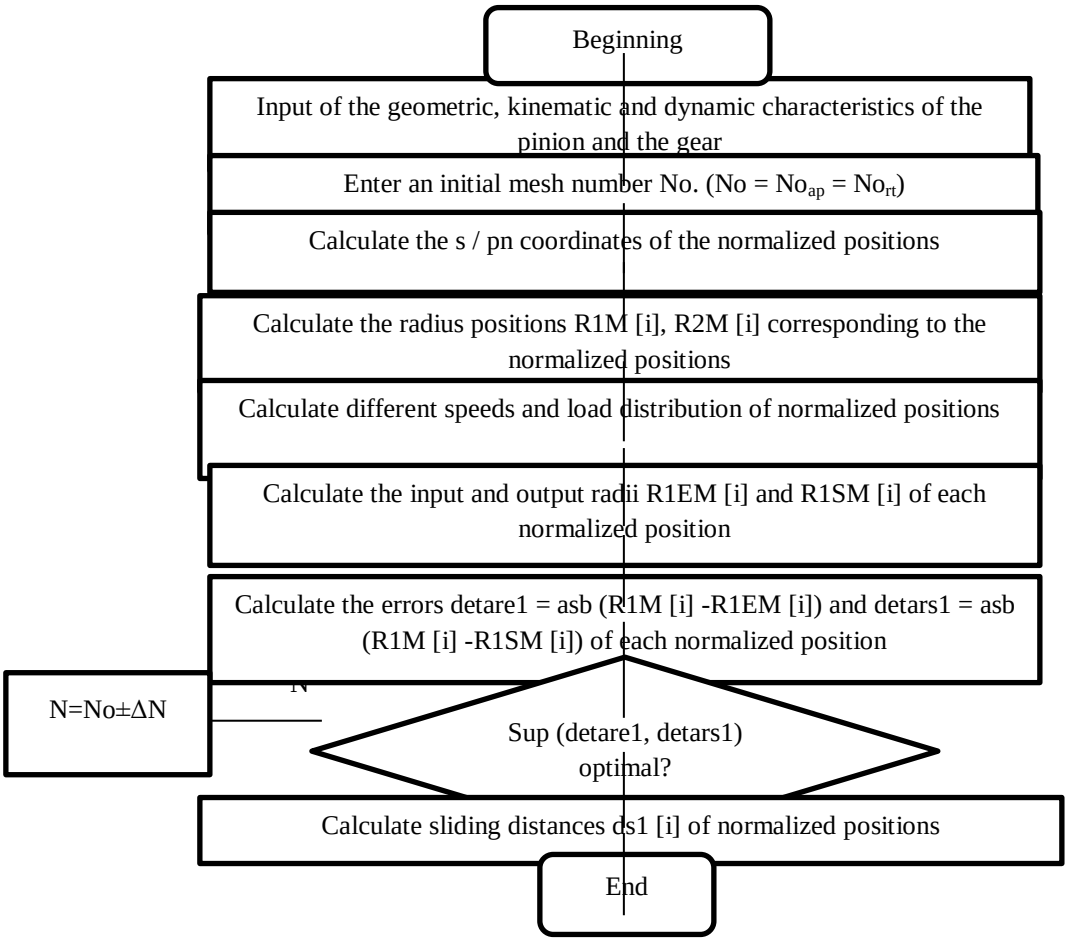

Figure 13:- Flowchart of the simulation program under Matlab

The flowchart of the Matlab simulation program is shown in Figure 13.

Below we do the simulation with materials commonly used in the field of plastic gears such as nylon, acetal and UHMWPE as well as our new composite material studied HDPE40B.

Table 2:- Characteristics of materials

Parameters	Materials			
	Uhmwpe	**Nylon**	**Acetal**	**Hdpe40b**
Specific weight: ρ	941.12 Kg/m^3	1140 Kg/m^3	1410 Kg/m^3	1185.6 Kg/m^3

Young modulus: E	0.68 GPa	2.85 GPa	2.6 GPa	3.45 GPa
Poisson coefficient $\boldsymbol{\upsilon}$:	0.41	0.4	0.3	0.33
Thermal conductibility k:	0.6747w/m.K	0.250W/m.K	0.228W/m.K	0.7870 W/mK
Specific heat : C	2301.2J/Kg.K	2750J/Kg.K	1470 J/Kg.K	1325.104 J/Kg°K
Friction coefficient : μ	0.5	0.28	0.21	0.2

In order to compare the appearance of the results with the results of the experimental wear tests available in the literature, we use the same meshing characteristics as those of the tests.

Table 3:- Specifications for simulation.

Module : m=2mm or diametral pitch DP=12.7
Number of tooth : Z_1= Z_2=30
Pressure angle : α =20°
Tooth wide : B=17mm
Rotation speed : $\boldsymbol{\omega}_1$, $\boldsymbol{\omega}_2$=500 et 1000 tr/min
Torque : T = 2.5 à 16.1 N.m

Results and Applications:-

A computer program developed in Matlab code with our method made it possible to obtain the results presented in the graphs of figures 14 to 19 and tables 4 to 6 for the different combinations of materials and operating parameters. The results show that the two methods give very close values except at the neighborhoods of the pitch point and the points of the head and the foot.

With the new approach, a non-zero sliding distance is obtained at the pitch point.

The points of the profile of the driven gear in the vicinity of the outside radius vertex including the point of the vertex, have short sliding time because their contact takes place at the same time at the moment of the theoretical beginning at point A. Just after, they are the first to come out of contact starting with the point of the vertex. The phenomenon is the same for the points in the vicinity of the contact start point of the driver gear profile. The similar phenomenon occurs at the sudden mesh exit points in the vicinity of the driver gear tooth vertex and in the vicinity of the contact ending point of the driven gear profile. This explains a steep climb from the beginning of the curve and a steep descent also from the end of the curve. The big differences between the two methods are found in these areas. The relative error is 100% at the pitch point since the old method gives zero sliding distance at this point.

When we see the difference between the two methods from the curves and error evaluation in tables 4 to 6, we estimate that the impact of the improvement to the neighborhoods of the pitch point and the points of the head and foot that would bring the new approach in real applications will be notorious.

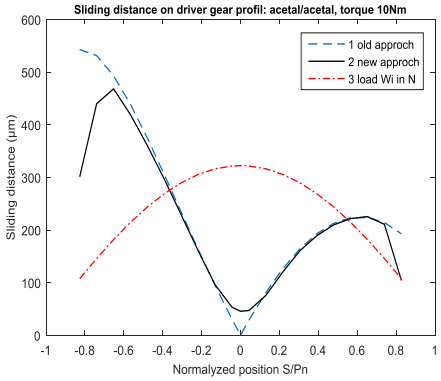

Figure 14:- Sliding distance on driver gear profile: acetal/acetal, T=10Nm, $\boldsymbol{\omega}_1$=1000rpm.

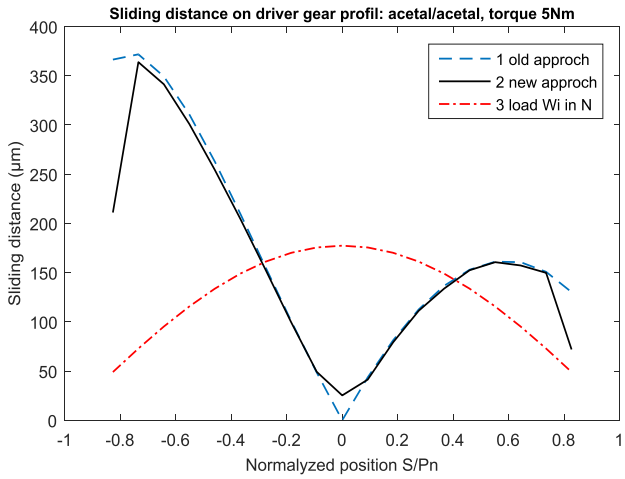

Figure 15:- Sliding distance on driver gear profile: acetal/acetal, T=5Nm, ω_1=1000rpm

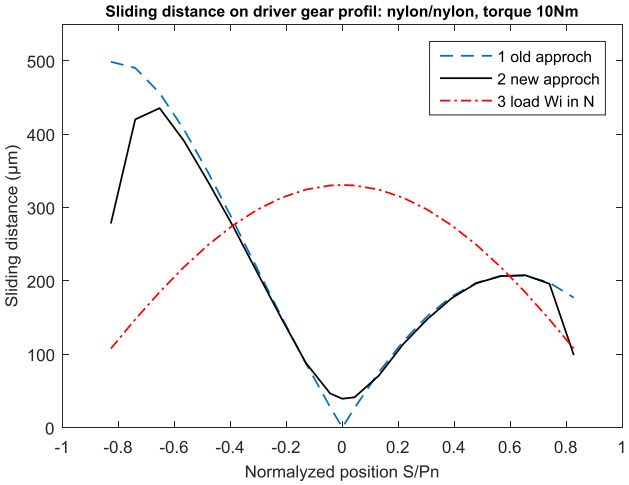

Figure 16:- Sliding distance on driver gear profile: nylon/nylon, T=10Nm, ω_1=1000rpm

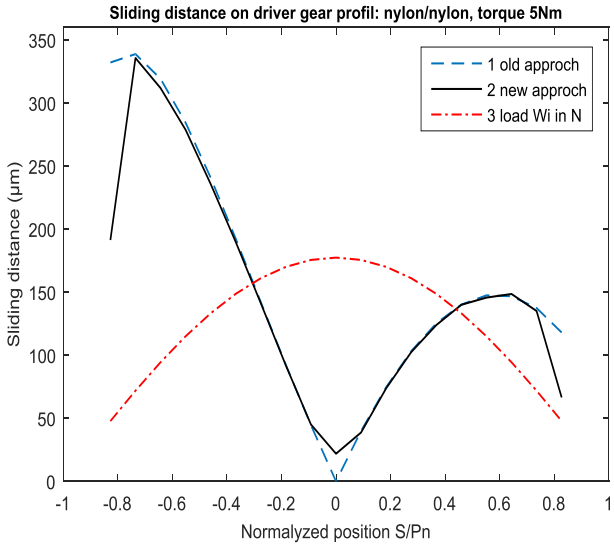

Figure 17:- Sliding distance on driver gear profile: nylon/nylon, T=5Nm, ω_1=1000rpm

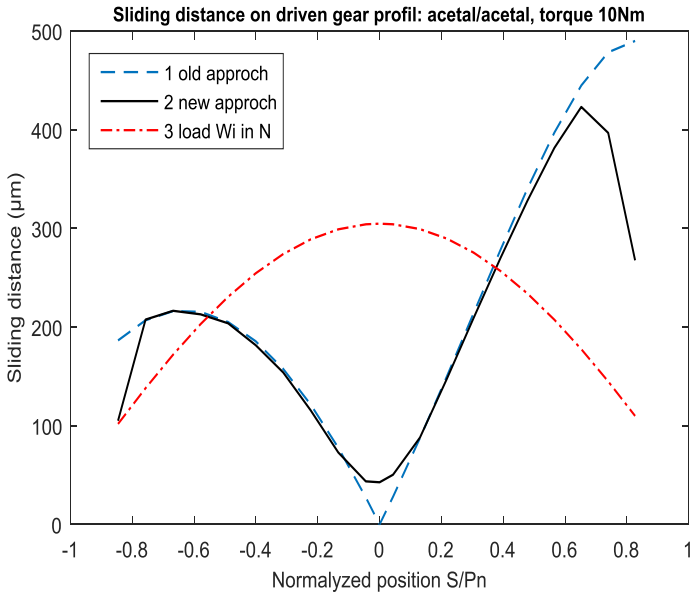

Figure 18:- Sliding distance on driven gear profile: acetal/acetal, T=10Nm, $\boldsymbol{\omega}_2$=1000rpm

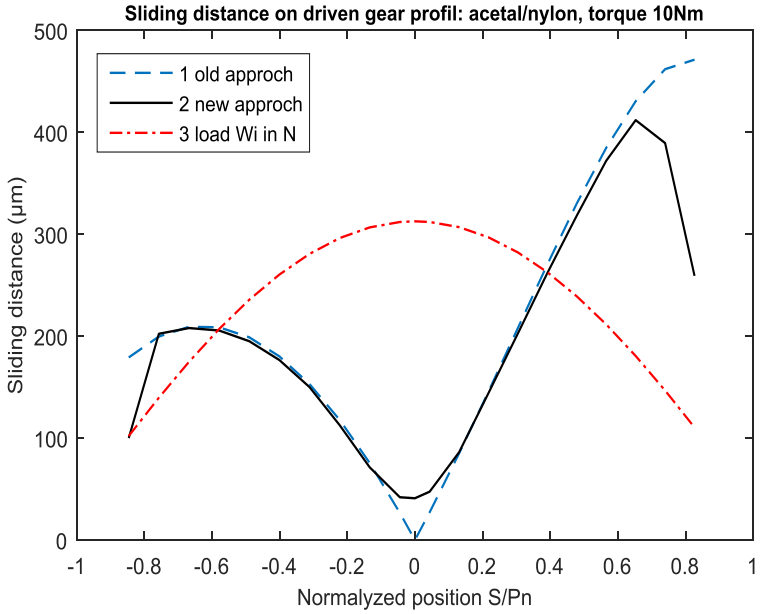

Figure 19:-Sliding distance on driver gear profile: acetal/nylon, T=10Nm, $\boldsymbol{\omega}_1$=1000rpm.

The relative error evaluation between the two methods for different meshing conditions is shown in tables 4 to 6.
Tableau 4- Sliding distance old approach dso1, new approach dsn1 and relative error Er between the two methods according to the normalized positions for acetal/acetal and T=10N.m driver gear.

Sliding distance (µm) dso1, dsn1, error Er(%) for acetal/acetal, Z1=Z2=30, T=10N.m, ω=1000rpm.											
Spn	-0.827	-0.740	-0.653	-0.566	-0.479	-0.392	-0.305	-0.217	-0.131	-0.044	0
dso1	542.79	531.26	493.00	438.53	374.37	304.98	233.64	162.82	94.48	30.21	0.00
dsn1	301.11	439.86	468.20	419.08	360.17	296.42	228.52	160.37	95.93	53.24	45.67
Er	80.26	20.78	5.30%	4.64%	3.94%	2.89%	2.24%	1.52%	1.51%	43.27	100

	%	%								%	%
Spn	0.044	0.131	0.217	0.305	0.392	0.479	0.566	0.653	0.740	0.827	
dso1	28.73	81.28	126.59	163.95	192.81	212.68	223.15	223.79	214.02	192.83	
dsn1	47.17	75.99	120.32	160.37	189.19	209.64	221.73	225.45	210.76	104.18	
Er	39.09 %	6.96%	5.20%	2.23%	1.91%	1.45%	0.64%	0.74%	1.55%	85.09 %	

Tableau 5:- Sliding distance old approach dso1, new approach dsn1 and relative error Er between the two methods according to the normalized positions for acetal/acetal and T=5N.m driver gear.

Sliding distance (µm) dso1, dsn1, error Er(%) for acetal/acetal, Z1=Z2=30, T=5N.m, ω=1000rpm.										
Spn	-0.827	-0.735	-0.643	-0.551	-0.459	-0.367	-0.276	-0.184	-0.092	0
dso1	366.41	371.75	349.28	310.72	262.78	209.83	154.98	100.58	48.44	0.00
dsn1	211.02	363.81	341.34	300.96	254.29	204.67	152.40	99.34	49.16	25.23
Er	73.63%	2.18%	2.33%	3.24%	3.34%	2.52%	1.70%	1.25%	1.47%	100%
Spn	0.092	0.184	0.276	0.367	0.459	0.551	0.643	0.735	0.827	
dso1	43.58	81.35	112.56	136.58	152.91	161.08	160.61	150.78	130.17	
dsn1	41.27	79.28	111.18	133.76	152.42	160.58	157.25	149.76	71.90	
Er	5.59%	2.61%	1.23%	2.11%	0.32%	0.31%	2.14%	0.68%	81.03%	

Tableau 6:- Sliding distance old approach dso1, new approach dsn1 and relative error Er between the two methods according to the normalized positions for nylon/nylon and T=10N.m driver gear.

Sliding distance (µm) dso1, dsn1, error Er(%) for nylon/nylon, Z1=Z2=30, T=10N.m, ω=1000rpm.											
Spn	-0.827	-0.740	-0.653	-0.566	-0.479	-0.392	-0.305	-0.217	-0.131	-0.044	0
dso1	492.62	490.22	456.07	406.33	347.27	283.13	217.01	151.29	87.81	28.08	0.00
dsn1	278.15	420.08	435.42	390.83	334.44	275.25	211.90	148.93	88.34	46.51	39.35
Er	79.26 %	16.70 %	4.74%	3.97%	3.83%	2.86%	2.41%	1.58%	0.60%	39.63 %	100 %
Spn	0.044	0.131	0.217	0.305	0.392	0.479	0.566	0.653	0.740	0.827	
dso1	26.71	75.54	117.62	152.28	178.99	197.28	206.76	207.02	197.49	177.13	
dsn1	41.29	70.92	113.91	148.19	176.69	196.74	206.44	207.77	196.08	98.87	
Er	35.32 %	6.52%	3.26%	2.76%	1.30%	0.27%	0.16%	0.36%	0.72%	79.17 %	

Conclusion:-

The sliding distance at the pitch point I is not zero in the actual meshing as assumed until our results to date. Due to the deformation of Hertz the point I comes into contact earlier when there is still a sliding speed and comes out of contact later when there is again a sliding speed.

Using the new approach to calculating the sliding distance allows us to use the Archard model-based wear law for the prediction of gear wear in plastic materials and their composites that have non-zero wear at the pitch point.

Bibliographie:-

1. KOFFI D. Analyse des méthodes de dimensionnement des engrenages en plastique, Note de veille technologique réalisée pour CETIM (Senlis) – France, 2004

2. Thaer OSMAN: Simulation de l'usure et d'avaries sur des dentures d'engrenages cylindriques - Influence sur le comportement statique et dynamique de transmissions par engrenages, Thèse de Doctorat, INSA de Lyon, 2012
3. KOFFI. D., ETUDE DU COMPORTEMENT THERMIQUE DES ENGRENAGES CYLINDRIQUES DROITS EN PLASTIQUE, Thèse de Doctorat (Ph.D.) en Génie Mécanique, Ecole Polytechnique de Montréal, Mars 1987
4. K. Mao, A new approach for polymer composite gear design: Mechanical Engineering, School of Engineering and Design, Brunel University, Uxbridge, Middlesex UB8 3PH, UK, ELSEVIER, Wear 262 (2007) 432–441.
5. K. Mao, W. Li, C.J. Hooke, D.Walton : Friction and wear behavior of acetal and nylon gears, ELSEVIER, Wear 267 (2009) 639-645.
6. Anders Flodin, Wear Investigation of Spur Gear Teeth: Machine Elements, Department of Machine Design, Royal Institute of Technology, Sweden
7. G.R. Nicolet, Conception et Calculs des Eléments de Machines, volume 3, Ecole d'Ingénieurs de Fribourg, juin 2006
8. Mathieu ROSSAT, Conception des transmissions de puissance : les Engrenages, Novembre 2014.
9. Dalia Jbily, Prise en compte de l'usure dans la modélisation du comportement sous charge des engrenages roues et vis tangentes Thèse de doctorat: Université de Lyon, 2016.
10. ZHAO et al, Integrated prognostics method for failure time prediction of gears subject to surface wear failure mode. Article in IEEE Transactions on Reliability. Jan. 2018.
11. ZHAO et al, An Integrated prognostics method under time-varying operating conditions, Article in IEEE Transactions on Reliability; vol 64, No2, PP 673 – 686. Jan. 2015.
12. Jun ZHANG et Xianzeng, Effects of misalignment on surface wear of spur gears, ARCHIVE Proceedings of the Institution of Mechanical Engineers Part J Journal of Engineering Tribology 1994-1996 (vols 208-210). March 2015.
13. MUNDE RAHUL M. et D. P. KAMBLE, Experimental investigation and FEA of wear in gear at torque loading conditions, IJARIIE-ISSN(O) 2395 – 4396; Vol-3 Issue -4 2017.